IMPROVING THE MECHANICAL RELIABILITY OF A TURBINE-COMPRESSOR-EXPANDER USED IN A NITRIC ACID PLANT

by

Darayus Pardivala

Technical Support Engineer

Hickham Industries Inc.

LaPorte, Texas

LeEllen Phelps

Maintenance Engineer

Apache Nitrogen Products Inc.

Benson, Arizona

and

Malcolm E. Leader

Turbomachinery Consultant

Applied Machinery Dynamics Company

Dickinson, Texas

Darayus Pardivala is a Technical Support Engineer at Hickham Industries Inc., in LaPorte, Texas. Mr. Pardivala received his B.S.M.E. and M.S.M.E. degrees from Texas A&M University. While at Texas A&M University, Mr. Pardivala worked for three years at the Turbomachinery Laboratory on the design and implementation of a large scale test facility to simulate and study unsteady flows found in turbomachinery. At Hickham Industries, he is responsible for resolving design related problems on all types of turbomachinery, which often include rotordynamic and performance studies. He also provides engineering support for all phases of turbomachinery repair including balancing and assembly procedures and specifications.

LeEllen Phelps graduated from University of Arizona (1987) with a B.S. in Energy Engineering. Ms. Phelps subsequently worked for a small mechanical engineering consulting firm in Tucson, Arizona.

Most recently, Ms. Phelps worked as a Project Engineer and the Maintenance Engineer at Apache Nitrogen Products, Inc. in Benson, Arizona. Her work there included heavy involvement with turbomachinery, pumps, boilers, piping, and heat exchangers.

Malcolm E. Leader is the Owner and Chief Engineer of Applied Machinery Dynamics Company in Dickinson, Texas. This company, founded in 1986, provides consulting services to users of rotating equipment. These services include lateral and torsional rotordynamics analysis, finite element analysis, journal bearing analysis, design and optimization, field engineering, balancing and alignment of rotating equipment, training, and general machinery problem solving. Prior to operating his own business, Mr. Leader was employed by Monsanto Company as a Rotating Equipment Engineer Specialist.

Mr. Leader graduated from the University of Virginia with a B.S.M.E. (1977) and an M.S.M.E. (1978). He is the author of numerous technical papers on bearing design and turbomachinery design and operation. He is a member of ASME, NSPE, TSPE, Sigma Xi, and the Houston Chapter of the Vibration Institute. He is a registered Professional Engineer in the State of Texas.

ABSTRACT

The repair of a turbine-compressor-expander to improve its mechanical reliability is described. The machine is unique, with two open-faced centrifugal compressor impellers in the center, three steam turbine stages overhanging on one end of the rotor and a radial hot gas expander overhanging on the other end, all connected with curvic couplings. The machine operates at 18,500 rpm and is used in the production of 300 tons per day of nitric acid. The plant has two identical units, one serving as a spare unit while the other is in service. The two modules are designated as serial number 1 (SN-1) and serial number 2 (SN-2). Ever since their first acquisition in 1978, SN-1 has proven to be more reliable than SN-2. While SN-1 has suffered four failures, SN-2 has suffered 13 failures, six of which have been while the rotor was being field balanced and/or passing through its first bending critical. The other failures can be attributed to various system failures at the plant.

Each failure was followed by an overhaul, the extent of which depended upon the amount of damage caused, but no serious consideration was ever given to improving the overall reliability of the machine. By the end of 1992, it was decided that the condition of the machine had deteriorated to the point where it could not be returned to service with a regular overhaul. Additionally, the reliability of the machine had to be improved. A detailed rotordynamic analysis was considered imperative to understanding the nature of the machine. Critical rotor compo-

nents were manufactured to replace existing ones. A detailed balancing procedure was adopted, and a mock-assembly was performed to set assembly clearances accurately prior to the final assembly. A shop balancing and assembly manual was written to closely control the entire overhaul.

The rotordynamic study and procedures adopted to improve the reliability of the machine are described. Also included are the actual startup data. The repair procedures have proven extremely successful, as can be seen from a comparison of the startup data before and after the overhaul. Vibration amplitudes at startup, as the machine passes through its first bending critical speed, are lower than seen previously. The machine was installed in November 1993, and has been shut down and started numerous times. Each time the machine has come up to operating speed without any problems, indicating that the overall mechanical reliability of the machine has been significantly improved.

The presented procedures can be easily adapted to improve the mechanical reliability of other machines with similar problems.

INTRODUCTION

The complete turbine-compressor-expander module is shown in Figure 1. A photograph of the rotor, assembled for its "as received" inspection, is shown in Figure 2. The machine is used at a nitric acid plant for air compression. The steam turbine, overhung on one end, and the radial hot gas expander, overhung on the other end, provide the power required to drive the compressor wheels located inboard of the bearings. Downstream of the module is a NO_x compressor-expander module. The hot gas leaving the expander of this module is used to drive the downstream NO_x module.

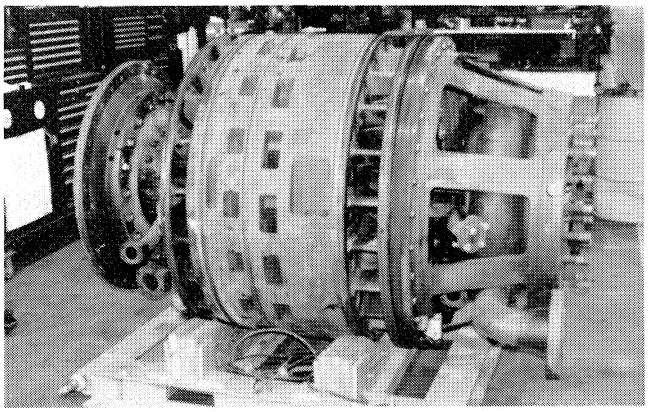

Figure 1. Complete Turbine-Compressor-Expander Unit.

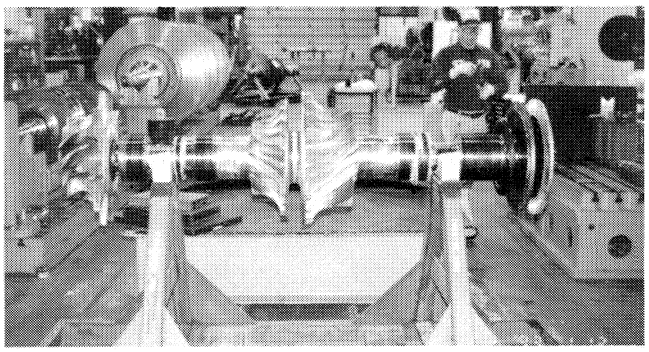

Figure 2. Rotor Assembled for the "As Received" Inspection.

A cross sectional view of the rotor is shown in Figure 3. The center body of the rotor consists of two open-faced, back-to-back, titanium centrifugal compressor impellers bolted between two 15Cr-5Ni precipitation hardened stainless steel stub shafts. At its operating speed of 18,500 rpm, the tip speed of the first stage compressor impeller is 1766 ft/s. Titanium, with its low density, is thus an appropriate choice in lowering the radial and tangential stresses due to centrifugal forces. The seal sleeves on the stub shafts, and between the two back-to-back compressor impellers are manufactured from 17Cr-4Ni precipitation hardened stainless steel. Both 15Cr-5Ni and 17Cr-4Ni precipitation hardened stainless steels provide high strength as well as excellent corrosion resistance and stability at operating temperatures.

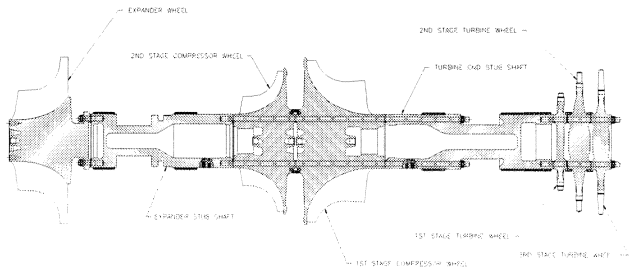

Figure 3. Cross Section of the Rotor.

Overhung on one end of the rotor is a radial expander, manufactured from A-286 alloy steel. A-286 is an iron based super-alloy providing excellent tensile strength at elevated temperatures up to 1300°F. The temperature of the gas at the inlet of the expander is 1200°F, making the A-286 an ideal choice of material.

The other end of the rotor has three axial turbine wheels manufactured from AISI 422 stainless steel. The first and second stage turbine blades are manufactured from AISI 422 stainless steel, while the third stage blades are manufactured from Inconel 718. All the components have curvic couplings and are held together by three sets of bolts manufactured from Inconel 718. The materials used in the manufacture of this rotor are an indication of the high mechanical and thermal stresses the rotor is subjected to in service.

The construction of the machine requires the steam turbine wheels and the radial expander to be assembled to the rotor center body in the case, making the assembly of the rotor and the rest of the machine extremely difficult.

HISTORY

Two air compressor modules were received from the original equipment manufacturer (OEM) in January 1978. The serial number 2 (SN-2) module was first installed May 5, 1978. A six month plant testing and debugging process ensued. In November 1978, the module was removed and sent to the OEM for repairs due to a second stage compressor wheel tip failure.

The module was returned to Apache Nitrogen Products five months later, with modifications to the design of the compressor wheel. It was installed in April 1979. It required five field balance runs at 14,000 rpm, with no full speed trim performed. The module was used for one month of production until it was removed and shipped back to the OEM for repairs. There was rub damage throughout the module, probably caused by a process valve failure.

After a six month repair cycle, the module was returned. During numerous balance runs, the shutdown delay for high vibrations was increased from one to three seconds because of

problems associated with getting through the first bending critical. The bearings failed during one of the balance runs.

Once again, the module was removed and shipped to the manufacturer for repair of rub damage throughout the module. The manufacturer recommended a high speed pit balance, but due to financial considerations, and the fact that the rotor would have to be disassembled before installation into the casing, the user company declined.

The module was next installed June 1980. Only four field balance runs, with one high speed trim adjustment, were required. It was in production for two months until the bearings failed, two days after a lube oil low pressure trip.

After another six month repair cycle, the module was installed in 1981. Then, after a six run field balance, with one final high speed trim adjustment, the plant tripped two hours after light off. Disassembly at the OEM revealed an expander wheel inducer tip failure. A new expander wheel was installed. At this point, the user company had two months total production on this module out of three years of ownership. Even though the other module, SN-1, had experienced problems, SN-2 had proved to be much more unreliable.

The SN-2 module was returned with the new expander wheel in August 1981. It failed during field balance while going through the first bending critical. There was rub damage throughout.

When the module was reinstalled in April 1982, the field balance took ten runs, but no full speed trim work was required. Apache finally got seven months of production out of the module before it failed going through critical after a surge. There was rub damage throughout, and a crack in the expander wheel.

In August 1983, SN-2 was received with a trimmed expander wheel. The field balance took six runs. It stayed in production until February 1984, when it was removed because of excessive steam consumption, and since the OEM was no longer in business, sent to another repair facility for the overhaul.

The work included tightening up critical clearances and the installation of metal spring energized seals throughout the casing between process streams. In April 1985, the field balance went well with five balance runs. The module saw 19 months of production before it was removed in November 1986 because of a thrust failure. The new repair facility was out of business by this time, so Hickham Industries Inc. was contacted for the repairs. As usual, there was rub damage throughout. There were also cracks in both titanium compressor wheels. Another crack was removed from the exducer portion of a vane on the expander wheel, with material removal matched at 180 degrees.

After a routine installation and balance in March 1987, the unit was in production for six weeks before experiencing another thrust failure. Fortunately, this time it was not a catastrophic failure, but there was an increase in rotor vibration level to 4.0 mils, which was beyond the trip point. The next production run lasted 13 months when, in August 1988, parts from the air intake silencer fell into the first stage compressor impeller, bending one blade and cracking another. The rotor was unstacked, the vanes fixed, and the journals were undercut and rechromed.

Once reinstalled in December 1988, the rotor was field balanced with great difficulty. The unit was in production for three months when it was removed due to sensitivity to changes in oil temperature. Disassembly revealed cracks in the second stage compressor wheel and the rotor was bowed. After repairs, which included complete unstacking the rotor to relieve the bow, the module was sent back to the user, stored (never installed or balanced), and then sent back to Hickham Industries Inc. to install a new expander wheel.

In March 1990, the module was installed and balanced. As in the last field balance, the rotor unbalance response was not linear. Even though the machine proved difficult to balance, once balanced, it performed with a record 18 month production run. It was removed from service in September 1991 due to worn expander inlet nozzles and failed compressor interstage seal. Disassembly revealed extensive damage due to high temperature exposure on the steam end and a rub on the expander wheel. After repairs, the module was installed in May 1992. The machine was brought down due to a shift in one of the curvic couplings. At this point, the condition of the machine had deteriorated to the point where it could not be returned to service with a regular overhaul. It was thus decided to make a major financial investment towards a complete engineered overhaul of the machine. The engineered overhaul started with a rotordynamic study to understand the nature of the machine. What followed were a thorough rotor balance and assembly procedure, and a mock assembly to carefully adjust clearances throughout the machine.

Described below are the rotordynamic analysis, and the procedures used to repair the machine. Also included are the startup data after the overhaul.

ROTORDYNAMIC ANALYSIS

Rotor Modelling

The most obvious difference between this rotor and most turbomachinery, is the construction in stacked sections. Early in the modelling process it was decided to ignore any flexibility in the joints. The rotor consists of an expander wheel, two compressor wheels, three steam turbine wheels and two hollow shaft sections. Each item was carefully measured and weighed including the 30 through bolts and nuts. Transverse and polar moments of inertia were calculated for each piece from the measurements. For the open bladed expander wheel and compressor wheels, an effective stiffness diameter was calculated and the external blade weights were added to those sections. For the steam turbine wheels, the disks were modelled as integral sections with the weights and inertias of the blades added at the appropriate points. The two compressor wheels in the center of the rotor are made of titanium, so these sections have a modified modulus of elasticity and density. All of the other components are steel, with the exception of the third stage turbine blades and the through bolts, which are made of Inconel 718. The model was assembled and double checked to assure a dimensional and weight match with the actual stacked rotor. The computer generated shaft cross section is shown in Figure 4. The centerlines of the journal bearings are marked as well as the rotor center of gravity. The center of gravity is necessary to calculate the radial loading on each of the journal bearings.

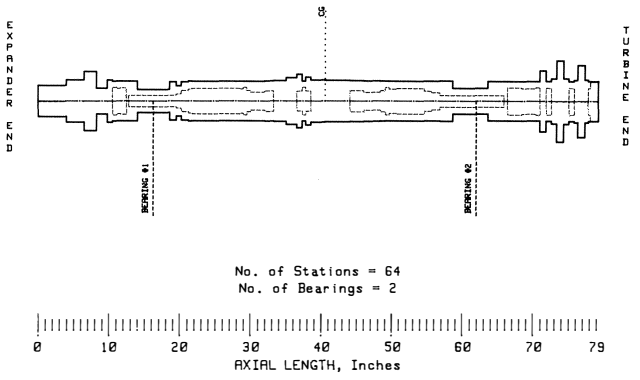

Figure 4. Computer Model of Rotor.

Undamped Mode Shape Analysis

The undamped critical speeds and mode shapes are generated to facilitate the understanding of the dynamic behavior of the rotor-bearing system. The seals and the aerodynamics contribute significantly to the actual vibration response. In this portion of the analysis, only the stiffness of the hydrodynamic bearings are considered. A single stiffness of 400,000 lb/in was chosen for each bearing, based on an average of the vertical and horizontal stiffnesses calculated for the tilting pad bearings.

An undamped critical speed map, which shows the first four natural frequencies as a function of support stiffness, is shown in Figure 5. The calculated stiffness values of the tilting-pad bearings are overlaid on the plot. The intersection of a stiffness with a natural frequency yields a critical speed. In this case, there should be two horizontal and two vertical frequencies for each of the first two modes. The frequency of the third mode is constant for each stiffness and the fourth mode is well above operating speed.

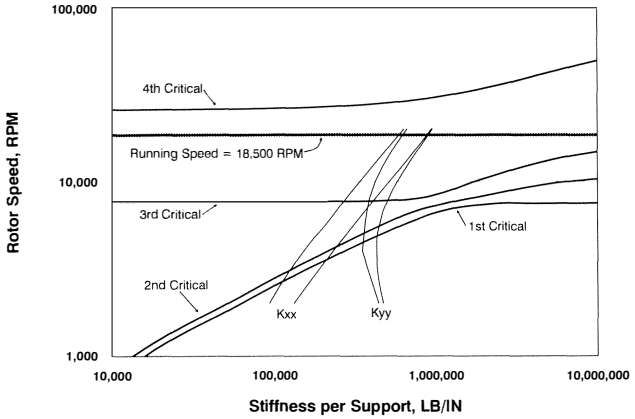

Figure 5. Undamped Critical Speed Map.

The mode shape plots are nondimensional in amplitude, since the forcing function is undefined for the undamped analysis. A view of the first critical speed mode shape is shown in Figure 6 at a frequency of 4,734 rpm. This mode is pivotal due to the double overhung nature of the design. There is a nodal point near the center of the rotor and high amplitude at each end of the machine. The amplitude at the bearings is approximately 50 percent of the maximum amplitude. The mode shape is shown in Figure 7 of the second mode at 5,314 rpm. This mode is cylindrical in shape, with the expander end amplitude slightly higher than the turbine end. The amplitude at the bearings is approximately 80 percent of maximum. The more relative amplitude present at the bearings, the more effective the fluid film damping. In this case, the first two modes are well damped from synchronous vibration.

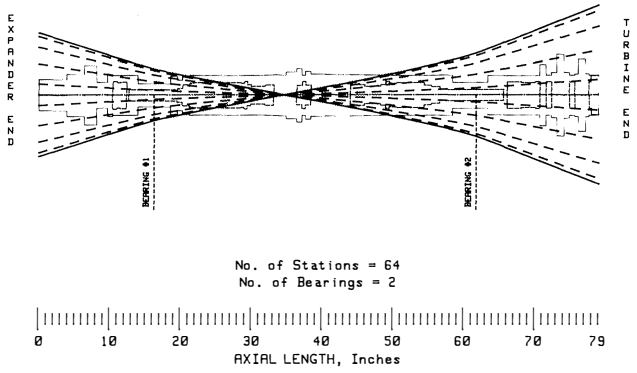

Figure 6. First Undamped Critical Speed Mode Shape at 4,734 RPM.

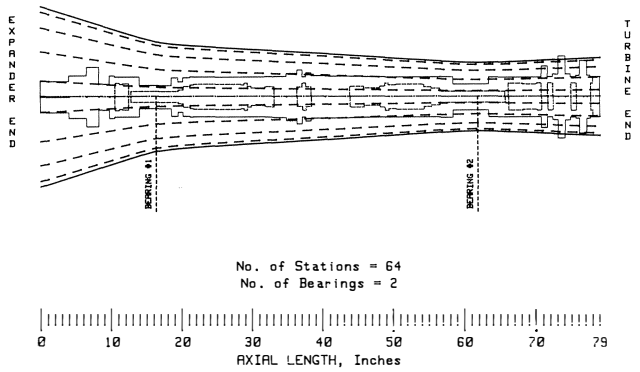

Figure 7. Second Undamped Critical Speed Mode Shape at 5,314 RPM.

The third mode, at 7,952 rpm, is shown in Figure 8. This mode shape is significantly different due to the proximity of nodal points to the bearing centerlines. With low relative amplitude in the hydrodynamic film, there is much less effective damping available to control vibration. There is higher relative amplitude inboard of the bearings in the area occupied by the labyrinth seals, which add important system damping to control this resonant speed.

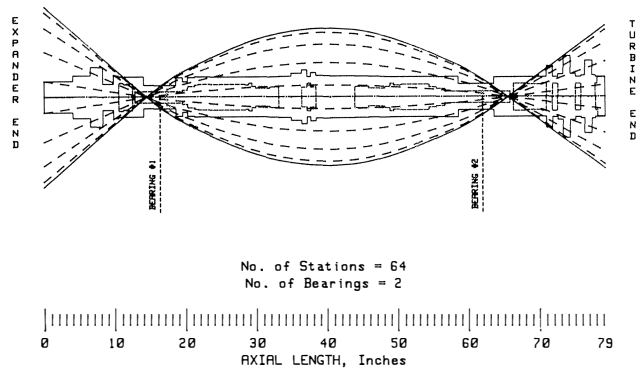

Figure 8. Third Undamped Critical Speed Mode Shape at 7,952 RPM.

Tilting Pad Bearing Analysis

The bearings in this machine are five pad, load-on-pad, tilting pad bearings. The pads are centrally pivoted on a line contact. The rest of the bearing dimensions are given in Table 1. The principal stiffness values are plotted as a function of speed in Figure 9. The vertical (Kyy) stiffnesses are higher than the horizontal (Kxx) stiffnesses and the expander end bearing is stiffer than the turbine end bearing. The principal damping values are plotted in Figure 10. Above 5,000 rpm, the horizontal and vertical damping values are nearly equal with the expander end bearing damping slightly higher than the turbine end bearing damping. The cross coupled stiffness and damping values are negligible and are not included in this analysis.

Table 1. Bearing Dimensions.

Bearing Factor	*Expander End Bearing*	*Turbine End Bearing*
Diameter	4.0 Inches	4.5 Inches
Axial Length	1.625 Inches	1.875 Inches
Pad Bore	0.0075 Inches	0.009 Inches
Preload	20%	20%

Labyrinth Seal Analysis

The primary contribution from the labyrinth seals is in the form of principal damping. These seals cover approximately nine inches of shaft on each end of the machine on both sides of both journal bearings (Figure 11). The labyrinth teeth are on shaft sleeves and mate to spring backed stationary carbon rings. The method used to calculate the dynamic damping values included the pressure drop across each set of teeth, the geometry of each tooth set and the properties of the gases. The seals were assumed to be centered. The principal damping values are plotted in Figure 12, where it can be seen that the seals are providing nearly as much damping as the bearings. For the third mode, almost all of the effective damping is from the labyrinth seals.

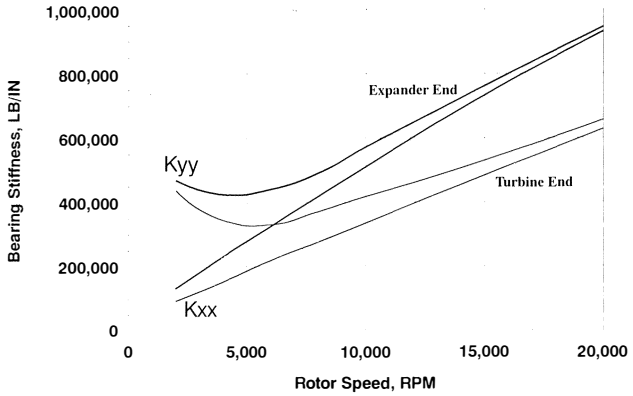

Figure 9. Tilting-Pad Bearings. Principal Stiffness Coefficients.

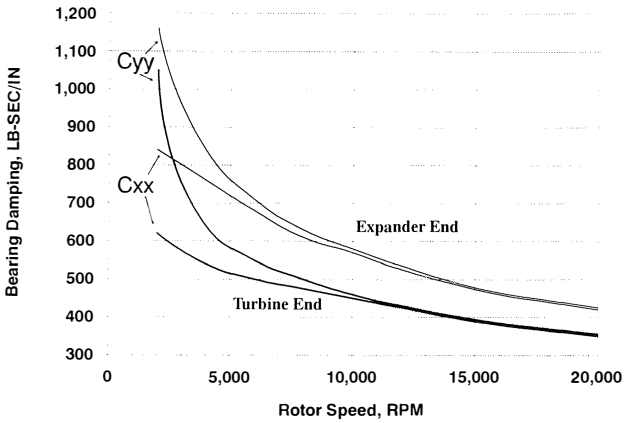

Figure 10. Tilting-Pad Bearings. Principal Damping Coefficients.

Unbalance Response Analysis

This portion of the analysis employs all the stiffness and damping coefficients from the bearings and seals. A reasonable

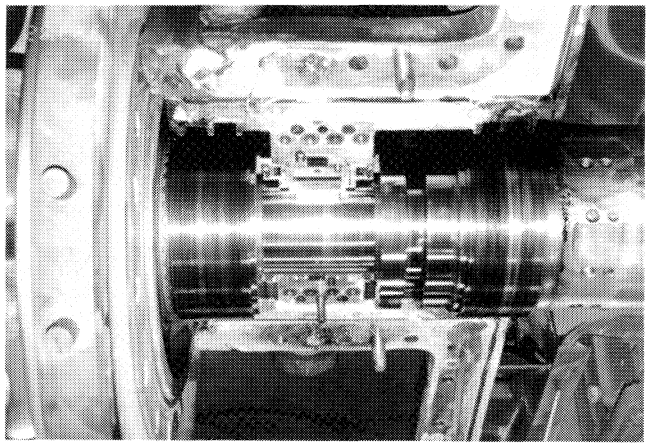

Figure 11. Expander End Stub Shaft and Bearing.

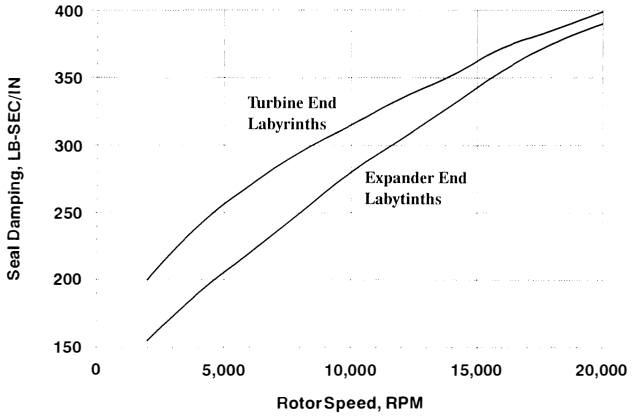

Figure 12. Labyrinth Seal. Principal Damping Coefficients.

set of imbalances were placed at five locations along the rotor, sufficient to match the proximity probe amplitudes observed in actual field operation. This imbalance distribution was designed to excite the first three critical speeds.

The predicted amplitude and phase are shown in Figure 13 as a function of speed for the expander end horizontal probe which is located 30 degrees in the direction of rotation from the horizontal splitline. The first two critical speeds are completely

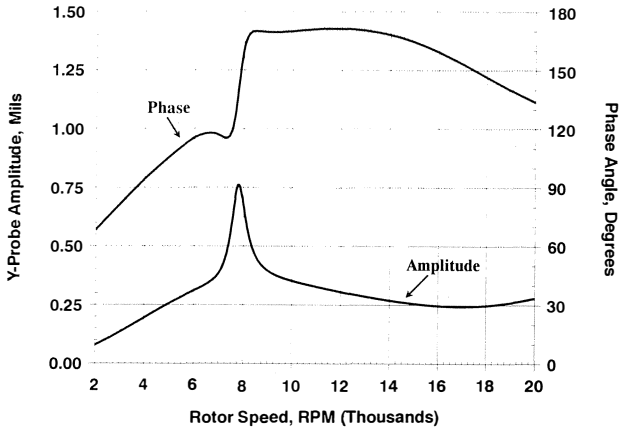

Figure 13. Predicted Unbalance Response at Expander End Horizontal Probe Location.

damped and the first peak response occurs at the third mode at 7,900 rpm. The calculated amplification factor at this location is 9.8. No other resonances are present up to 20,000 rpm. This plot closely matches the experimental amplitude shown in Figure 14.

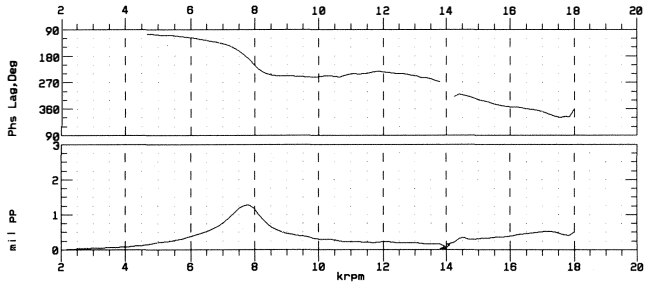

Figure 14. Startup Amplitude and Phase from the Expander End Horizontal Proximity Probe.

A similar plot is shown in Figure 15 for the vertical probe on the turbine end of the machine. Again, only the response of the third mode is visible, with a calculated amplification factor of 12 closely matching the experimental data sets.

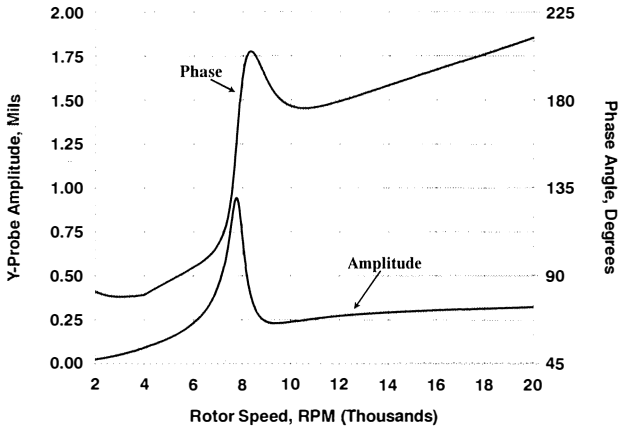

Figure 15. Predicted Unbalance Response at Turbine End Vertical Probe Location.

One of the objectives of this analysis was to predict the maximum amplitudes along the entire length of the rotor in order to set seal clearances as close as possible. This was important to maximize efficiency and avoid rotor to stator contact. Shown in Figure 16 are the absolute shaft amplitude values at 7,800 rpm as a function of axial rotor length. The ends of the rotor have much higher amplitude than the center of the machine. A similar calculation was done for full speed conditions and is shown in Figure 17. From this information, a table of minimum and maximum clearances was generated for use during assembly.

Stability Analysis

The subsynchronous excitation of each of the first three modes was examined to complete the analysis. This problem had never occurred in operation and was considered a minor part of the total analysis. The primary difficulty is estimating the aerodynamic cross coupling. All stability calculations showed positive logarithmic decrements and no stability problems were anticipated.

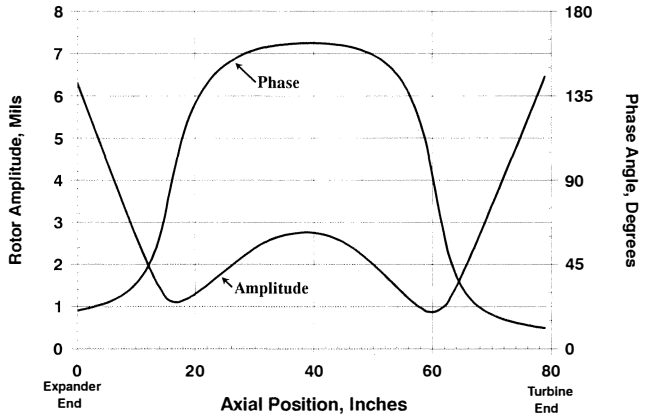

Figure 16. Absolute Amplitude and Phase Along Length of Rotor at 7,800 RPM.

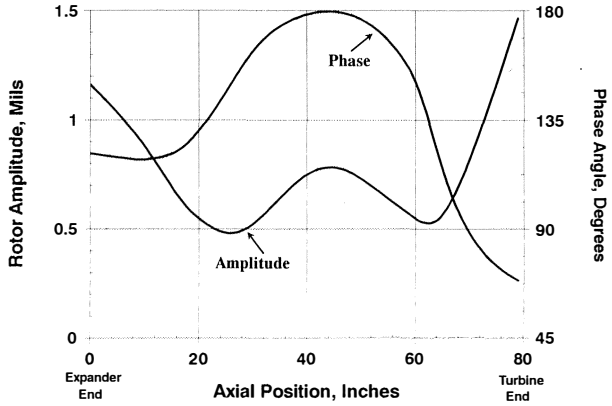

Figure 17. Absolute Amplitude and Phase Along Length of Rotor at 18,500 RPM.

ROTOR MANUFACTURE, ASSEMBLY AND BALANCE

Accurate assembly and balancing of the rotor is critical to the optimum performance of a turbomachine. The rotor in this case has seven sets of curvic couplings held together by three sets of tie bolts. Thus, close attention needs to be paid to the assembly of the rotor to obtain optimum runouts and balance. In this case, an additional concern is that the first bending critical of the rotor has nodal points at the bearing journals, resulting in a very lightly damped mode. Close control of the balancing of the rotor is, therefore, imperative for the successful operation of the machine. The procedures detailed in this section can be used for other rotors having similar characteristics.

Flexible rotors can be defined as rotors that do not always stay balanced at high speeds after they have been balanced at low speeds. Rotors of this nature are at times balanced at running speed in a vacuum chamber, while closely monitoring the displacement of the rotor as it passes through a natural frequency. This method eliminates the possibility of a failure at startup all the way to the running speed of the rotor, even when the rotor passes through a natural frequency. The subject rotor runs well above its first bending mode and had a history of failing as it passed through its first bending critical speed.

The assembly of the machine requires the expander wheel and turbine wheels to be disassembled from the rotor before it can be installed in the case. After careful consideration, it was decided

that balancing the rotor in a vacuum chamber at high speed would not be beneficial, since the rotor would have to be disassembled prior to inserting it into the case. The changes in the rotor due to reassembly in the case would be sufficient to negate the precise corrections made in the high speed balance pit. Instead, it was decided to do a thorough component and progressive low speed balance on the rotor. Final trim balancing on the rotor would be done in the field.

The center body of the rotor was removed from the case, and the entire rotor was reassembled. The "as received" runouts and balance were checked on the rotor (Figures 2 and 18). The runouts indicated that the rotor was bowed. It was thus decided that the entire rotor had to be disassembled, and the curvic faces had to be closely inspected. The curvic faces were blue checked for contact, and it was found that the contact between a number of the faces was not adequate. To further investigate the cause of the bow in the rotor, the axial runouts on the compressor wheel curvic faces were also checked.

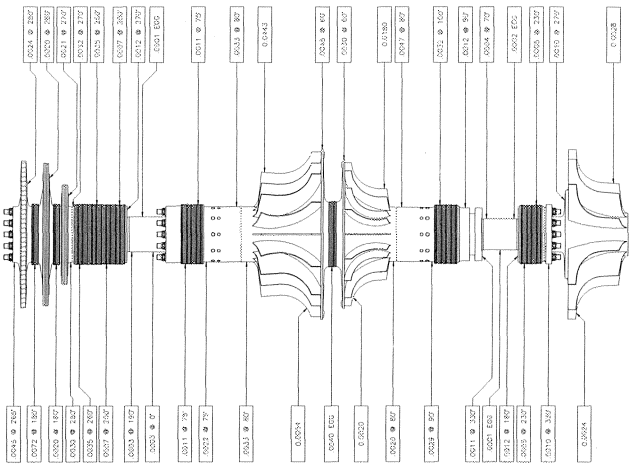

Figure 18. "As Received" Runouts on the Rotor.

Inspecting the axial runouts on components with curvic faces requires specialized equipment, since the axial runouts need to be measured on the mating surfaces. During the initial manufacturing process, a special set of curvic "masters" are manufactured to extremely tight tolerances. All curvics cut, are initially checked to these masters. Axial runout measurements are made on each component with the component placed between a set of curvic masters.

In the absence of the curvic masters, the axial runouts on the compressor wheels were individually mapped on a coordinate measuring machine. The axial runout was found to be around 0.003 in, which was considerably greater than the 0.0005 in tolerance set for these parts. The results found using the masters were in agreement with these results. A decision was made to skim grind (0.005 in per curvic face maximum) all the curvic faces to get them within tolerance. The shortening of the rotor resulting from the grinding would be compensated for by the manufacturing of slightly oversized stub shafts.

Each stub shaft has two rows of correction holes used to balance the rotor. The smaller set of holes is used for shop balance while the second set is used for field balancing. During prior repairs on the rotor, it was found that the weights added in the correction holes were not sufficient to balance the rotor. Permanent corrections on the stub shafts by metal removal were thus necessary in the past to obtain the balance tolerance set for the rotor. The condition of the stub shafts, coupled with the axial runout problems, provided sufficient justification for the manufacture of the new oversized stub shafts. The rest of the curvic faces were skim ground to improve the contact between the mating curvic faces.

Component Balancing

Special balance mandrels with curvic faces and several sets of match weighed through bolts and nuts were manufactured for component balancing. Each mandrel was dynamically balanced individually before balancing the components.

Accurate component balancing is the key to a well balanced rotor. For the two compressor impellers and stub shafts, the initial imbalance readings were taken with each component mounted between the balancing mandrels. Runouts were recorded on the component mounted between the mandrels, and the initial imbalance readings were obtained. Permanent corrections were made on the inner diameters of the components after removing the mandrels. The locations of the balance planes in the component balance are shown in Figure 19. The planes were carefully chosen to minimize the effects of the material loss. Each component was then placed between the mandrels and the balance was checked. The procedure was repeated until the residual unbalance in each component was well below the tolerance. The first stage turbine wheel is shown in Figure 20 mounted between the mandrels for the component balance. The new expander end stub shaft is shown in Figure 21 being checked for runouts between the balance mandrels. Two critical observations were made during the component balancing:

- The permanent balance corrections were made on the components by metal removal. The mandrels were then bolted back on and the components were run up again in the balance machine to check the balance. Repeatability of the balance reading was a major problem, especially on the titanium impellers. It was then realized that the small amount of heat generated during the metal removal was deflecting the curvic faces and preventing proper seating with the mandrels. The deflection of the curvic faces was not apparent in the runout checks. Results were repeatable once the part was kept at room temperature for around one hour after the metal removal process.

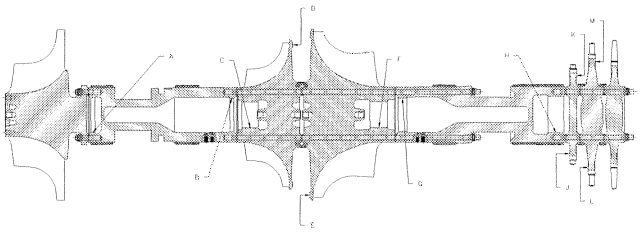

Figure 19. Correction Planes for the Component Balance.

- The 17Cr-4Ni precipitation hardened stainless steel labyrinth seal sleeves on the stub shafts are assembled with an interference of 0.017 in (the stub shaft outside diameter is 7.000 inches). During the assembly of the sleeves, the runouts were closely monitored and no changes of shaft runout greater than 0.0002 in (any phase) were allowed. It was however noticed, that even though the shaft runouts were in tolerance, a couple imbalance was induced in the shaft if the sleeves were not perfectly seated. The sleeves were flame heated in the balance stand and the component was rotated until it cooled to room temperature. The procedure was repeated if the imbalance in the shaft after assembling each sleeve was greater than two times the final

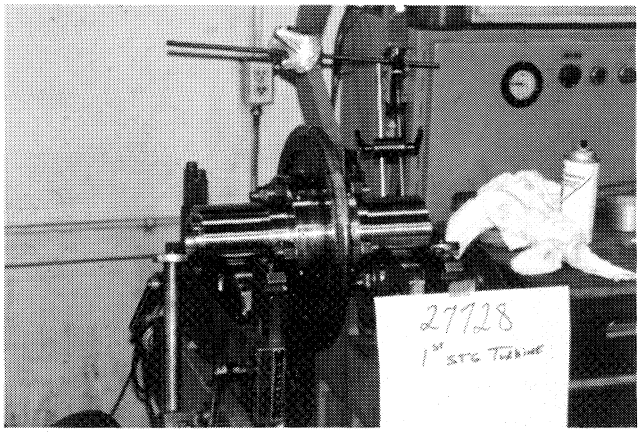

Figure 20. First Stage Turbine Wheel Mounted Between Mandrels for the Component Balance.

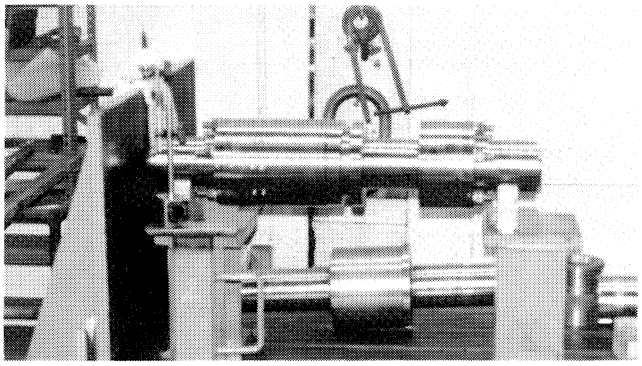

Figure 21. New Expander End Stub Shaft Being Checked for Runouts Between Balance Mandrels.

balance tolerance for that stub shaft. This step is crucial, since it is imperative to minimize the residual stresses in the rotor body.

The first and second turbine wheels were also balanced between the balance mandrels, but only a single plane correction was made due to the narrow width of the wheels. The third stage turbine wheel and the expander wheel were not individually balanced as they are the outermost components on each end of the rotor and would be balanced in the progressive stacking.

Rotor Assembly and Progressive Balancing

After the component balancing was complete, the next step was to progressively assemble and balance the rotor. The center body of the rotor was assembled, as shown in Figure 22, and runouts were checked. Even with the newly ground curvic couplings, the runouts obtained were not satisfactory. The runouts were projected in two planes to obtain the true shape of the rotor. Using this method, the curvic faces that were not seated correctly were identified. The curvics were then rotated based on the data and the rotor was stacked again. It is important to remember that grinding the curvic faces does not necessarily result in low runouts on the rotor, and that optimum stacking of the curvic couplings is necessary to obtain the appropriate runouts. The final set of runouts obtained for the center body of the rotor are also shown in Figure 22. The assembly was then weighed, the balance tolerance calculated per API specifications, and balanced by adding weights in planes III and IV (see Figure 23 for balance planes).

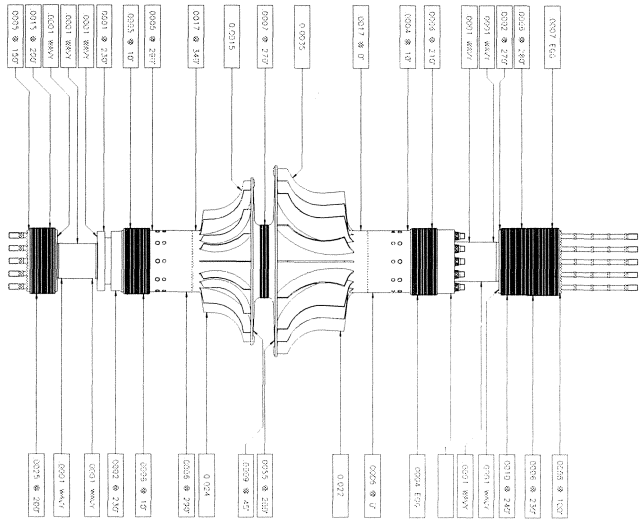

Figure 22. Progressive Balance Runouts Number 1. Center Body of the Rotor.

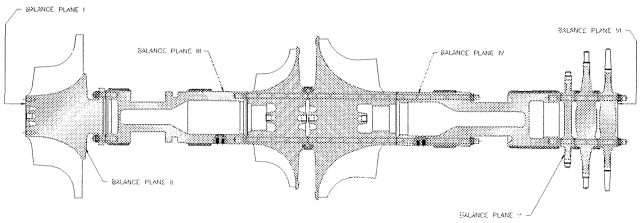

Figure 23. Corrections Planes for the Progressive Balance.

The balance machine was then set up to read the imbalance in planes I and II. The residual imbalance of the rotor was thus transposed to planes I and II. The expander wheel was then assembled, and the runouts and balance were checked (Figure 24). The residual imbalance of the rotor center body (projected to planes I and II) was subtracted from the readings to obtain the actual imbalance due to the addition of the expander wheel. The expander wheel was then rotated by 180 degrees and the proce-

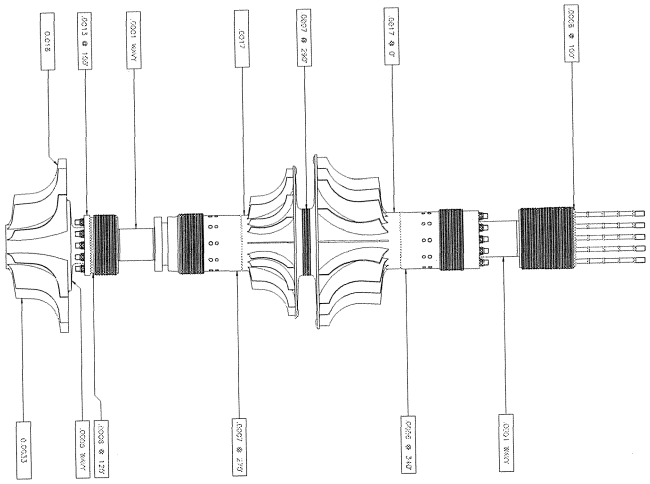

Figure 24. Progressive Balance Runouts Number 2. Expander Wheel Assembled.

dure repeated. The optimum position of the expander wheel was then determined by the procedure explained by Jackson [1]. The balance corrections on the expander wheel were reduced by 45 percent using this method. The balance tolerances were calculated based only on the weight of the expander wheel. The residual imbalance of the rotor projected to planes I and II was vectorially subtracted out of the final balance readings.

The imbalance of the assembly (center body and expander wheel) was then projected to balance planes V and VI, and the readings recorded. The first stage turbine wheel was then assembled using match weighed aluminum spacers, as shown in Figure 25. A static correction was made on the wheel using balance mud. No permanent correction was made by removing metal, since the correction plane coincided with plane V (one of the two planes used in the final 2-plane correction for the overhung turbine wheels). The second stage wheel was then assembled, as shown in Figure 26, and a permanent single plane correction was made by removing metal from the wheel. Each time the balance correction was reduced using the method described by Jackson [1]. The third stage wheel was then added, the balance machine set up to read planes V and VI, and final corrections were made. The balance tolerances were calculated based on the overhung weight of the turbine wheels. Again, the residual imbalance of the rest of the rotor assembly projected to planes V and VI was vectorially subtracted from the balance readings to obtain the correct imbalance values. After the overhung ends were balanced, a final trim was made on the rotor in planes III and IV. Final runouts on the entire rotor (Figure 27) and the mechanical and electrical runouts on the probe locations were charted.

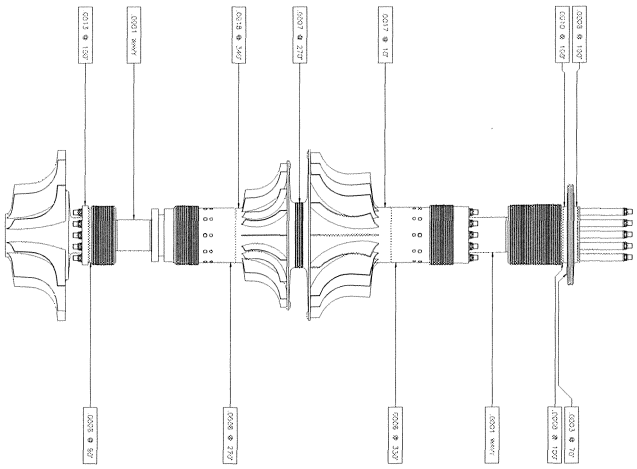

Figure 25. Progressive Balance Runouts Number 3. First Stage Turbine Wheel Assembled.

The importance of correctly assembling and balancing rotors in high speed turbomachinery cannot be overemphasized. Close attention needs to be paid to every detail. All blades in this case that were weld repaired or replaced, were weighed and charted by computer to provide the minimum imbalance obtainable. Close attention was also paid to bolt stretch, nondestructive testing and handling of all components. The methods described above have resulted in a rotor that has performed more reliably and consistently than before. Field balancing is not as great a risk anymore and was done within two corrections.

FINAL ASSEMBLY

The complete rotor was set in the bottom half of the case and all axial and radial clearances were checked. All case adjustments necessary due to the rotor modification were made at this time. The design of this machine requires the expander and turbine wheels to be disassembled from the rotor before the expander volute and turbine housing can be bolted on. The rotor is then assembled in the case. Once the clearances were adjusted, the turbine wheels and expander wheel were carefully match marked and disassembled from the rotor. The rest of the assembly was then completed, with the expander and turbine wheels assembled on the rotor at the appropriate time, paying close attention to the match marks and bolt stretch. It is imperative for the curvics to be seated identically to when the rotor was balanced. Any variation in the mating of the curvic faces will result in balance variations on the rotor.

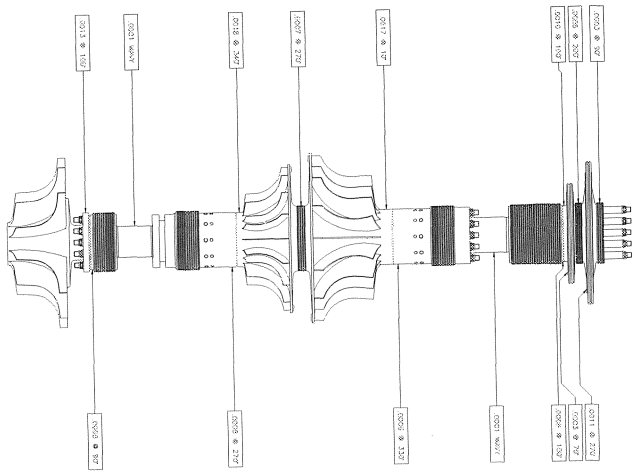

Figure 26. Progressive Balance Runouts Number 4. Second Stage Turbine Wheel Assembled.

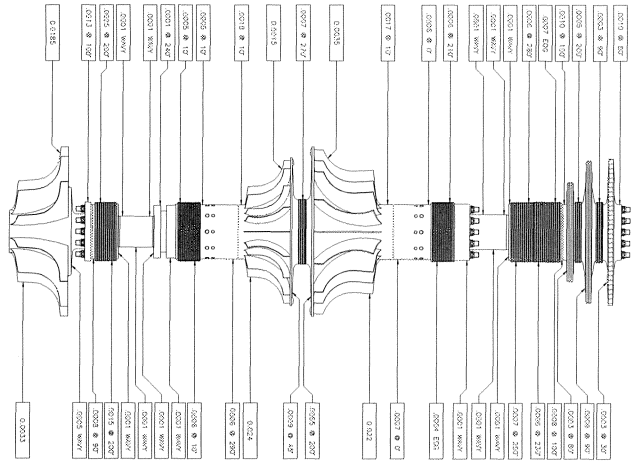

Figure 27. Progressive Balance Runouts Number 5. Complete Rotor Assembled.

FIELD DATA COLLECTION

The sets of amplitude and phase data points collected from the displacement probes fitted to this machine consist of startup runs. This is due to the fact that it is far more likely to have a planned startup than a planned shutdown. In order to evaluate the internal mechanical health of a machine, transient data points must be collected from slow roll to full speed. The vibration signals were gathered with a computer based system that monitored and stored amplitude and phase vectors from all

four proximity probes, along with the waveforms used to generate frequency spectrums. These sets of data are then plotted as a function of rotor speed. In all of the following plots, the only visible peak is the third critical speed at 7,800 rpm. Neither of the first two rigid body modes are manifested, nor are there any other critical speed rotor resonances up to 18,500 rpm.

The synchronous amplitude and phase collected from the expander end horizontal probe during a 20 second startup from slow roll to the balance speed of 14,000 rpm is plotted in Figure 14. After balancing, the speed was increased to 18,500 rpm. From this plot, an amplification factor of 7.1 can be calculated. This is lower than the predicted amplification factor of 9.8, but that is often the case when comparing the actual and theoretical unbalance responses of a rotor that is accelerating. This is favorable to the turbomachinery user, since it encourages conservative design. It is important to note that the slow roll runout value of 0.26 mils at nine degrees was vectorially subtracted from each point on this plot. This is the only way to assure accurate evaluation of the amplification factor.

A similar plot for the turbine end vertical probe location is shown in Figure 28. The calculated amplification factor is 9.2 for this critical speed peak. Again, this is lower than the predicted amplification factor.

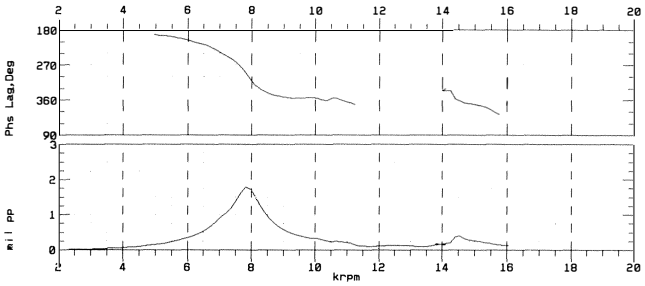

Figure 28. Startup Amplitude and Phase from the Turbine End Vertical Proximity Probe.

Additional information is available from the transient data sets. These measurements are also from the turbine end vertical probe. A spectrum is generated every 750 rpm and combined as a cascade plot in Figure 29. This plot shows that the primary vibration component is synchronous. There is no evidence of any subsynchronous vibration, and the lack of twice running speed vibration is convincing testimony to the integrity of the rotor construction and absence of any internal misalignment. There is an interesting ten times vibration component that is easily explained as a minute distortion of the probe surface area from the force of the ten main body through-bolts.

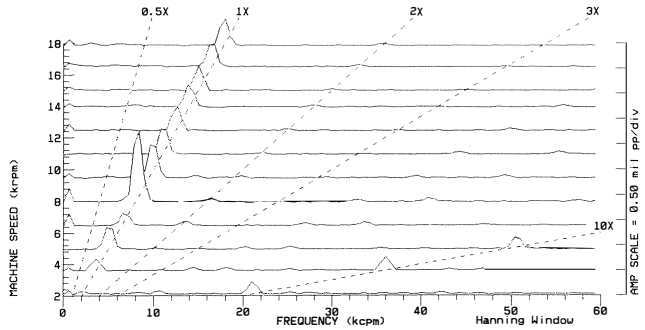

Figure 29. Cascade of Spectrums from the Turbine End Vertical Proximity Probe During Startup.

Finally, it is informative to examine the orbits generated from the orthogonal probes. The horizontal and vertical signals are combined in Figure 30 to show shaft centerline orbits from 2,100 rpm to 12,450 rpm. These orbit are the unfiltered vibration signal and clearly show a nearly circular orbit, even at resonance. This is additional evidence that there are no significant internal forces or preloads. All of the vibration levels in these plots are low. This means that this machine not only operates with low stress levels, but also is able to repeatedly traverse a potentially damaging bending mode critical speed without damage.

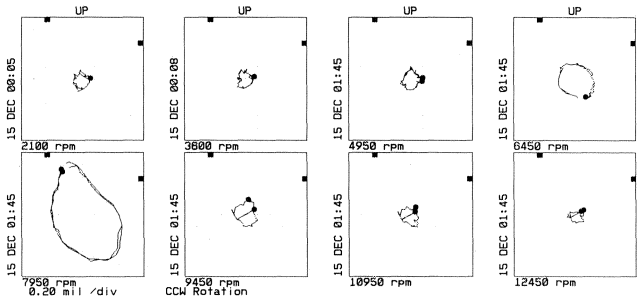

Figure 30. Orbits from the Turbine End Proximity Probes During Startup.

For comparison, a typical startup plot from the SN-1 module, expander end horizontal displacement probe is shown in Figure 31. This rotor runs well at operating speed, but has difficulty in passing through the first bending critical. The rotor is also extremely difficult to field balance.

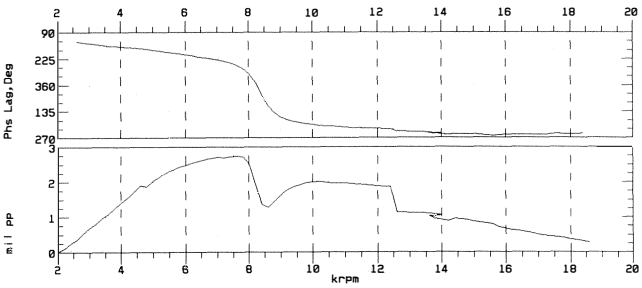

Figure 31. Typical Startup Plot From the SN-1 Module, Expander End Horizontal Displacement Probe.

CONCLUSIONS

The problem machine addressed herein is a unique high speed builtup rotor that had exhibited repeated high vibration, rubs and mechanical failure. Replacement parts and rebuilds failed to adequately solve these problems. A unified approach consisting of a thorough understanding of the rotordynamic behavior, combined with exacting measurements, extremely careful shop balancing and assembly, precision tolerances, and high speed field balancing has resulted in the desired smooth operation. The steps outlined are not necessary for every machine, but the concepts are applicable to any machine during an overhaul or modification. The transient field plots presented validate the intense engineering and mechanical efforts needed to achieve the successful end result.

REFERENCES

1. Jackson, C., "Single Plane Balancing," *Proceedings of the Eighth International Pump Users Symposium,* Turbomachinery Laboratory, Texas A&M University, College Station, Texas, pp. 105-127 (1991).

ACKNOWLEDGEMENTS

The authors would like to thank John East, Peter Alexander, Barney McLaughlin, John Babb, Joe Burkhart, Danny Riggs, and Mark Bounds at Hickham Industries Inc. for their invaluable assistance. They would also like to thank William Trbula, Bryan Bounds, and Paul Peterson for their exceptional work on the balancing and assembly of the module. Finally, they would like to express their sincere gratitude to Charles Jackson for keeping them on the right track with his engineering insight and frequent memos faxed mostly between midnight and 6:00 a.m.